PHYSICAL REVIEW A VOLUME 58, NUMBER 3 SEPTEMBER 1998

Homodyne measurements on a Bose-Einstein condensate

J. F. Corney and G. J. Milburn
Department of Physics, The University of Queensland, Queensland 4072, Australia
(Received 24 December 1997)

We investigate a nondestructive measurement technique to monitor Josephson-like oscillations between two spatially separated neutral atom Bose-Einstein condensates. One condensate is placed in an optical cavity, which is strongly driven by a coherent optical field. The cavity output field is monitored using a homodyne detection scheme. The cavity field is well detuned from an atomic resonance, and experiences a dispersive phase shift proportional to the number of atoms in the cavity. The detected current is modulated by the coherent tunneling oscillations of the condensate. Even when there is an equal number of atoms in each well initially, a phase is established by the measurement process and Josephson-like oscillations develop due to measurement backaction noise alone. [S1050-2947(98)03509-4]

PACS number(s): 03.75.Fi, 05.30.Jp, 32.80.Pj

I. INTRODUCTION

The experimental observation of Bose-Einstein condensation (BEC) in dilute systems of trapped neutral atoms [1–4] has stimulated a large research program on Bose-Einstein condensation of dilute neutral atom gases in confining potentials. One aspect of BECs that has attracted much theoretical work is the idea of phase. Several papers [5–7,10,11] have discussed the role of measurements in establishing the phase, in the form of interference between two condensates or Josephson-like coherent tunneling between the condensates. The latter situation is discussed in this paper, where we investigate homodyne detection of the output of an optical cavity containing one condensate in a double well system. The measurement process induces tunneling oscillations though backaction noise and thus induces a phase difference between the two separated parts of the condensate. In a self-consistent manner, the tunneling imposes a phase modulation on the light field, which is detected in the homodyne current.

II. CONDENSATE MODEL

The model of the condensate used here, namely, the BEC in a double-well potential, has been presented in previous papers [12], and so we only present a brief overview of the system here. The potential is symmetric with barrier height and well separation chosen so that only two single-particle states are below the barrier separating the two wells. This enables a treatment of the many-body problem with a two-mode approximation. The resulting model is sufficiently simple to enable an analytic solution to be found for the semiclassical equations, and to permit a tractable numerical comparison of the semiclassical description with the full quantum dynamics.

Consider a dilute gas of atoms moving in the double-well potential $V(\mathbf{r})$ with

$$V(\mathbf{r})=b\left(x^2-\frac{d}{2b}\right)^2+\frac{1}{2}m\omega_t^2(y^2+z^2), \tag{1}$$

where the interwell coupling occurs along x, and ω_t is the trap frequency in the y-z plane. This potential has elliptic fixed points at $\mathbf{r}_1=+q_0\mathbf{x},\mathbf{r}_2=-q_0\mathbf{x}$, where $q_0^2=d/2b$, at which the linearized motion is harmonic with frequency $\omega_0=(4d/m)^{1/2}$. We set $\omega_t=\omega_0$ for simplicity. It is convenient to scale the length in units of the position uncertainty in a harmonic oscillator ground state, r_0 where $r_0=\sqrt{\hbar/2m\omega_0}$. The barrier height is then given by $B=(\hbar\omega_0/8)(q_0/r_0)^2$.

The many-body Hamiltonian describing an atomic BEC in a confining potential is [13]

$$\hat{H}(t)=\int d^3\mathbf{r}\left[\frac{\hbar^2}{2m}\nabla\hat{\psi}^\dagger\nabla\hat{\psi}+V\hat{\psi}^\dagger\hat{\psi}+\frac{U_0}{2}\hat{\psi}^\dagger\hat{\psi}^\dagger\hat{\psi}\hat{\psi}\right], \tag{2}$$

where m is the atomic mass, $U_0=4\pi\hbar^2a/m$ measures the strength of the two-body interaction, and a is the s-wave scattering length. $\hat{\psi}(\mathbf{r},t)$ and $\hat{\psi}^\dagger(\mathbf{r},t)$ are the Heisenberg picture field operators, which annihilate and create atoms at position $\mathbf{r}$, and normal ordering has been used.

For a suitable choice of B, only two energy eigenstates lie beneath the barrier, which enables a many-body treatment in terms of only two single-particle states. For details we refer to [12]. We now define the state $u_0(\mathbf{r})$ as the normalized ground-state mode of the local potential $\tilde{V}^{(2)}(\mathbf{r})$, around the bottom of each well, with energy E_0, and define the local mode solutions of the individual wells $u_{1,2}(\mathbf{r})=u_0(\mathbf{r}-\mathbf{r}_{1,2})$. These local modes are approximately orthogonal with a first-order correction (ϵ^1) to orthogonality given by the overlap between the modes of opposite wells. The energy eigenstates of the global double-well potential may then be approximated as the symmetric $(+)$ and asymmetric $(-)$ combinations

$$u_\pm(\mathbf{r})\approx\frac{1}{\sqrt{2}}[u_1(\mathbf{r})\pm u_2(\mathbf{r})], \tag{3}$$

with corresponding eigenvalues $E_\pm=E_0\pm\mathcal{R}$, and

$$\mathcal{R}=\int d^3\mathbf{r}u_1^*(\mathbf{r})[V(\mathbf{r})-\tilde{V}^{(2)}(\mathbf{r}-\mathbf{r}_1)]u_2(\mathbf{r}). \tag{4}$$

The matrix element $\mathcal{R}$, which is of order ϵ^1, describes the coupling between the local modes. The tunneling frequency

Ω between the two minima is then given by the energy level splitting of these two lowest states:

$$\Omega = 2\mathcal{R}/\hbar = \omega_0 \frac{q_0^2}{2r_0^2} e^{q_0^2/2r_0^2}. \tag{5}$$

In the two-mode approximation we expand the field operators in terms of the local modes and introduce the Heisenberg picture annihilation and creation operators

$$c_j(t) = \int d^3\mathbf{r} u_j^*(\mathbf{r}) \hat{\psi}(\mathbf{r},t) \tag{6}$$

so that $[c_j, c_k^\dagger] \approx \delta_{jk}$. The validity of this expansion if ensured when the overlap is small:

$$\frac{\mathcal{R}}{E_0} = \frac{\Omega}{\omega_0} \ll 1. \tag{7}$$

The ratio of the separation of the minima of the global potential $V(\mathbf{r})$ to the position uncertainty in the state $u_0(\mathbf{r})$ can be as small as $2q_0/r_0 = 6$ (as in the simulations presented in this paper), and this condition is still satisfied. The many-body Hamiltonian then reduces to the following two-mode approximation:

$$\hat{H}_2(t) = E_0(c_1^\dagger c_1 + c_2^\dagger c_2) + \frac{\hbar\Omega}{2}(c_1 c_2^\dagger + c_1^\dagger c_2) + \hbar\kappa[(c_1^\dagger)^2 c_1^2 + (c_2^\dagger)^2 c_2^2], \tag{8}$$

where $\kappa = U_0/2\hbar V_{\text{eff}}$, and $V_{\text{eff}}^{-1} = \int d^3\mathbf{r} |u_0(\mathbf{r})|^4$ is the effective mode volume of each well.

The two-mode approximation is valid when many-body interactions produce only small modifications of the ground-state properties of the individual potentials. This is true when

$$\hbar\omega_0 = \frac{\hbar^2}{2mr_0^2} \gg \frac{N|U_0|}{V_{\text{eff}}}. \tag{9}$$

Using $V_{\text{eff}} \approx 8\pi^{3/2} r_0^3$ for this case, we obtain the following condition on the number of atoms:

$$N \ll \frac{r_0}{|a|}. \tag{10}$$

The values used in our simulations, namely, $r_0 = 5$ μm, $a = 5$ nm, and $N = 100$ satisfy this criterion. Thus the two-mode approximation is valid for small number of atoms compared to current experiments with $N = 10^3 - 10^6$.

The first term in Eq. (8) may be removed by transforming to an interaction picture, resulting in the Hamiltonian

$$\hat{H}_2 = \frac{\hbar\Omega}{2}(c_1 c_2^\dagger + c_1^\dagger c_2) + \hbar\kappa[(c_1^\dagger)^2 c_1^2 + (c_2^\dagger)^2 c_2^2]. \tag{11}$$

A full quantum analysis of the quantum dynamics resulting from the many-body Hamiltonian Eq. (2) is not tractable, however, considerable insight can be gained within the two-mode approximation. In [12] an angular momentum model was defined, which is equivalent to the Hamiltonian Eq. (11). Using the transformations

$$\hat{J}_z = \frac{1}{2}(c_1^\dagger c_2 + c_2^\dagger c_1), \tag{12}$$

$$\hat{J}_x = \frac{1}{2}(c_2^\dagger c_2 - c_1^\dagger c_1), \tag{13}$$

$$\hat{J}_y = \frac{i}{2}(c_2^\dagger c_1 - c_1^\dagger c_2) \tag{14}$$

and setting $c_1^\dagger c_1 + c_2^\dagger c_2 = \hat{N} = N$ (as the total number is conserved), the Hamiltonian becomes

$$\hat{H}_2 = \hbar\Omega \hat{J}_z + 2\hbar\kappa \hat{J}_x^2. \tag{15}$$

Here we have neglected terms proportional to N and N^2 since they merely correspond to a shift in the energy scale. The Casimir invariant is

$$\hat{J}^2 = \frac{\hat{N}}{2}\left(\frac{\hat{N}}{2} + 1\right). \tag{16}$$

This is analogous to an angular momentum model with total angular momentum given by $j = N/2$.

The angular momentum operators have a simple physical interpretation. The operator $\hat{J}_z$ corresponds to the particle occupation number difference between the single-particle energy eigenstates. For example, the maximal weight eigenstate $|j,j\rangle_z$ corresponds to all the particles occupying the highest single-particle energy eigenstate, $\psi_2(x)$. The operator $\hat{J}_x$ gives the particle number difference between the localized states of each well. In fact the x component of the position operator in the field representation is

$$\hat{x} = \frac{2q_0}{N}\hat{J}_x. \tag{17}$$

Thus the maximal and minimal weight eigenstates of $\hat{J}_x$ correspond to the localization of all the particles in one well or the other.

III. HOMODYNE DETECTION SCHEME

Figure 1 illustrates the system under investigation here. One of the wells of the double-well system is placed in one arm of an optical cavity. The cavity is strongly driven by a coherent field at the cavity frequency. We assume that on the time scale of tunneling oscillations, the cavity is heavily damped. The cavity field thus relaxes to the steady state on a much faster time scale than the BEC dynamics. This enables us to make an adiabatic elimination of the cavity dynamics. The cavity field is assumed to be far off resonance with respect to a dipole transition in the atomic species. The effect of the atoms is then entirely dispersive and shifts the phase of the cavity field by an amount proportional to the number of atoms in the cavity at any particular time. If the atomic number in the cavity oscillates, so will the phase shift. Thus any tunneling of the condensate will be manifest in a modulated phase shift of the optical field exiting the cavity. To detect this phase shift we consider a homodyne detection scheme. The light leaving the cavity is combined with the

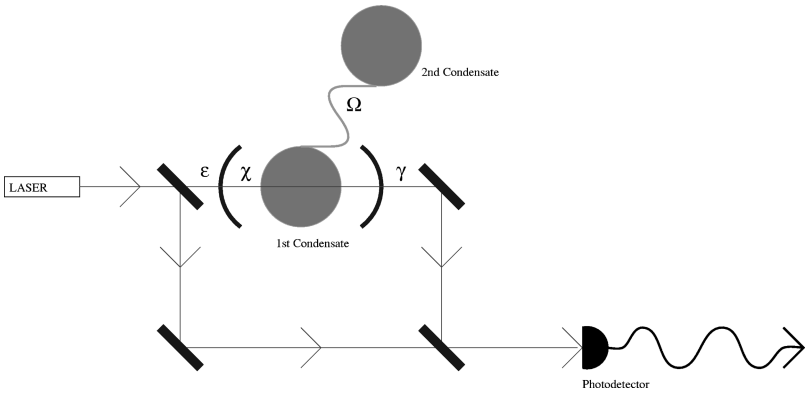

FIG. 1. Schematic representation of the homodyne detection scheme to monitor the tunneling between two spatially separated condensates. One part of the condensate is contained in an optical cavity. The light in the cavity is well detuned from the atomic resonance. The output light from the cavity is detected by balanced homodyne detection.

reference beam and allowed to fall on a photodetector, which records the photocurrent. If there is a difference in atom number of the two condensates, then coherent tunneling can occur and the homodyne current will be modulated at the tunneling frequency.

Assuming that the incoming light is detuned from any atomic resonance, the interaction Hamiltonian density is

$$\hat{\mathcal{H}}_I = \hat{\Psi}^\dagger(\mathbf{r})[\hat{H}_{\text{c.m.}} - \hbar\mu g(\mathbf{r}) a^\dagger a]\hat{\Psi}(\mathbf{r}), \tag{18}$$

where a, $a^\dagger$ are the cavity field operators, $g(\mathbf{r})$ is the intensity mode function, and $\mu = \Omega_R^2/4\Delta$, with Rabi frequency Ω_R and optical detuning Δ. $\hat{\Psi}(\mathbf{r})$ and $\hat{\Psi}^\dagger(\mathbf{r})$ are the atomic many-body operators, and $\hat{H}_{\text{c.m.}}$ describes the center-of-mass motion.

Introducing the condensate field operators c, $c^\dagger$ and averaging over the optical mode function gives the interaction energy:

$$\begin{aligned}\hat{H}_I &= -\hbar\chi a^\dagger a c_1^\dagger c_1 \\ &= -\hbar\frac{N}{2}\chi a^\dagger a - \hbar\chi a^\dagger a \hat{J}_x,\end{aligned} \tag{19}$$

where χ is the interaction strength. If the optical mode has a beam waist w, then the interaction strength can be written as

$$\chi = \frac{\sqrt{2}\mu}{\sqrt{2(r_0/w)^2 + 1}}. \tag{20}$$

For $N = 100$ atoms, $\chi > 10^{-3}\ \text{s}^{-1}$ should give detectable phase shifts (0.1 rad), and should be experimentally feasible. For example, with r_0 as above, $w = 30\ \mu\text{m}$, $\Delta/2\pi = 100$ MHz, saturation intensity $I_s = 17\ \text{W/m}^2$, optical frequency $\omega/2\pi = 3.8\times10^{14}$ Hz, atomic linewidth $\gamma_a/2\pi = 10^7$ Hz and incident power $P = 6$ mW, in a cavity 10 cm long, then $\chi \approx 10^{-2}\ \text{s}^{-1}$. Larger values of χ may then be achieved by reducing the detuning or the incident intensity.

The cavity is assumed to be driven by a strong coherent field of strength ϵ and strongly damped at the rate γ. Hence the master equation for the whole system is, with $\hbar = 1$,

$$\begin{aligned}\dot{\rho}_{\text{tot}} &= -i\Omega[\hat{J}_z, \rho_{\text{tot}}] - i2\kappa[\hat{J}_x^2, \rho_{\text{tot}}] \\ &\quad - i\left(\delta - \frac{N\chi}{2}\right)[a^\dagger a, \rho_{\text{tot}}] + i\chi[a^\dagger a \hat{J}_x, \rho_{tot}] - i\epsilon[a^\dagger \\ &\quad + a, \rho_{\text{tot}}] + \frac{\gamma}{2}(2a\rho_{\text{tot}}a^\dagger - a^\dagger a\rho_{\text{tot}} - \rho_{tot}a^\dagger a),\end{aligned} \tag{21}$$

where the initial cavity detuning $\delta = N\chi/2$ is chosen to re-

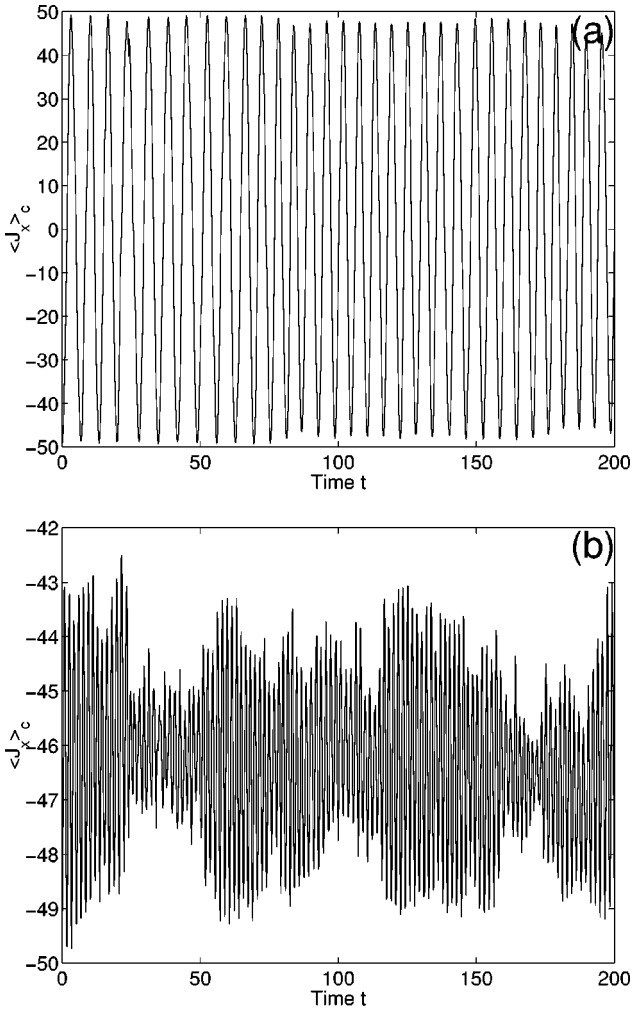

FIG. 2. Evolution of $\langle \hat{J}_x \rangle_c$ in the monitored system, for $N = 100$ atoms all initially in one well and $\overline{\chi} = 0.01$. In (a), $\overline{\kappa} = 0.005$ and in (b), $\overline{\kappa} = 0.02$.

move the N-dependent linear dispersion. The optical field may now be adiabatically eliminated from the master equation [14]:

$$\dot{\rho} = -i\Omega[\hat{J}_z,\rho] - i2\kappa[\hat{J}_x^2,\rho] + i\chi|\alpha|^2[\hat{J}_x,\rho] - D[\hat{J}_x,[\hat{J}_x,\rho]], \tag{22}$$

where the coherent amplitude is $\alpha = -2i\epsilon/\gamma$ and $D = 8\chi^2\epsilon^2/\gamma^3$. The double commutator represents a decoherence produced by photon-number fluctuations in the optical fields. It is a quantum measurement backaction term consistent with the interpretation that the optical field makes a measurement on the condensate. In fact this last term destroys coherence in the eigenbasis of $\hat{J}_x$ and thus should inhibit tunneling oscillations. This is indeed true for the ensemble of measured systems described by the master equation. However, as we show below, it is not true for a particular realization of a single measurement run. The ensemble-averaged effect of the measurement can be seen in the operator moment equations (for $\kappa = 0$):

$$\langle \dot{\hat{J}}_x \rangle = -\Omega\langle \hat{J}_y \rangle, \tag{23}$$

$$\langle \dot{\hat{J}}_y \rangle = \chi|\alpha|^2\langle \hat{J}_z \rangle + \Omega\langle \hat{J}_x \rangle - D\langle \hat{J}_y \rangle, \tag{24}$$

$$\langle \dot{\hat{J}}_z \rangle = -\chi|\alpha|^2\langle \hat{J}_y \rangle - D\langle \hat{J}_z \rangle. \tag{25}$$

The terms with coefficient $\chi|\alpha|^2$ produce a precession around the x axis, which tends to inhibit coherent tunneling. The effect of these terms can be negated by adding a linear ramp, or tilt, to the double-well potential. The D terms cause a decay toward the origin, indicating decoherence, as expected. If the system is started in a number state with an equal number of atoms in each well, then no tunneling will occur at all—these moments remain identically zero.

When the wells are tilted, so that the precession around the x axis is suppressed, we can obtain equations for the second order moments:

$$\langle \dot{\hat{J}}_x^2 \rangle = -\Omega\langle \hat{\Lambda} \rangle, \tag{26}$$

$$\langle \dot{\hat{J}}_y^2 = \Omega\langle \hat{\Lambda} \rangle + 2D(\langle \hat{J}_z^2 \rangle - \langle \hat{J}_y^2 \rangle), \tag{27}$$

$$\langle \dot{\hat{J}}_z^2 \rangle = 2D(\langle \hat{J}_y^2 \rangle - \langle \hat{J}_z^2 \rangle), \tag{28}$$

$$\langle \dot{\hat{\Lambda}} \rangle = 2\Omega(\langle \hat{J}_x^2 \rangle - \langle \hat{J}_y^2 \rangle) - D\langle \hat{\Lambda} \rangle, \tag{29}$$

where $\hat{\Lambda} = \hat{J}_x\hat{J}_y + \hat{J}_y\hat{J}_x$.

Thus even when the system is started with an equal number of atoms in each well, the unconditional evolution of $\langle \hat{J}_x^2 \rangle$ and $\langle \hat{J}_y^2 \rangle$ exhibit oscillations initially. For long times, the amplitude of these oscillations decays due to D and the system approaches the fixed point $\langle \hat{J}_x^2 \rangle = \langle \hat{J}_y^2 \rangle = \langle \hat{J}_z^2 \rangle$. From this we see that the condensate has on average a definite initial phase (which is clearly seen in the second-order moments, but not the first-order moments), which is determined by the initial state. In our simulations the initial state was chosen to be a eigenstate of $\hat{J}_x$, which is not the only state that gives an equal number of atoms in each well. Presumably in a real experiment, the initial state would be

$$|\psi(\tau)\rangle = e^{-i\tau\hat{J}_z}|j,0\rangle_x, \tag{30}$$

where τ is a random variable uniformly distributed on the interval $[0,2\pi]$. This then implies a random initial phase.

A common technique for dealing with master equations describing open systems in quantum optics is to numerically simulate stochastic realisations of quantum trajectories. This method has already been used by several authors investigating the effect of measurement on the relative phase of BECs [7–9], but these differ from the approach used here in that we monitor the homodyne detection current. The resultant stochastic process is a diffusive evolution rather than the jump processes that occur in the direct detection of atoms or individual photons. The quantum trajectory method is a very appropriate one for the situation considered in this paper. We have one two-part condensate system continuously monitored by the homodyne detection scheme. If there is any phase difference between the two parts of the condensate it will be established in each run of the experiment. The quantum trajectory method enables us to simulate each run of an experiment. The master equation, however, corresponds to an average over many runs of the experiment and many homodyne current records. For this reason moments calculated directly from the master equation will show no evidence of quantum tunneling if there is no initial phase difference between the condensates. In contrast, as we show, a single run of the experiment can establish a self-consistent phase difference even if no phase difference is present initially. Such a ''measurement induced'' phase difference is manifest in a measurement induced tunneling current.

The *conditional* master equation (that is the evolution conditioned on the measurement result) for the optical field undergoing homodyne detection is [15,16]

$$\left(\frac{d\rho_c}{dt}\right)_{\text{field}} = \gamma\mathcal{D}[a]\rho_c + \sqrt{\gamma}\frac{dW(t)}{dt}\mathcal{H}[a]\rho_c, \tag{31}$$

where $dW(t)$ is the infinitesimal Weiner increment. In this equation, ρ_c is the density matrix that is conditioned on a particular realization of the homodyne current up to time t. Wiseman's superoperators are defined as

$$\mathcal{D}[a]\rho = a\rho a^\dagger - \tfrac{1}{2}(a^\dagger a\rho + \rho a^\dagger a), \tag{32}$$

$$\mathcal{H}[a]\rho = a\rho + \rho a^\dagger - tr(a\rho + \rho a^\dagger)\rho. \tag{33}$$

The stochastic Shrödinger equation, which describes the conditional evolution of the system is

$$d|\tilde{\Psi}_c(t)\rangle = dt[-i\hat{H}_2 - i\hat{H}_1\,\tfrac{1}{2}\gamma a^\dagger a + I(t)a]|\tilde{\Psi}_c(t)\rangle, \tag{34}$$

where $\hat{H}_2 = \Omega\hat{J}_z + 2\kappa\hat{J}_x^2$ and $|\tilde{\Psi}_c(t)\rangle$ is the *unnormalized* ket describing the conditional state of the system. The measured current is $I(t) = \gamma\langle a + a^\dagger\rangle(t) + \sqrt{\gamma}\xi(t)$, where the stochastic term $\xi(t)$ has the correlations

$$\langle \xi(t)\rangle = 0, \tag{35}$$

$$\langle \xi(t),\xi(t')\rangle = \delta(t-t'). \tag{36}$$

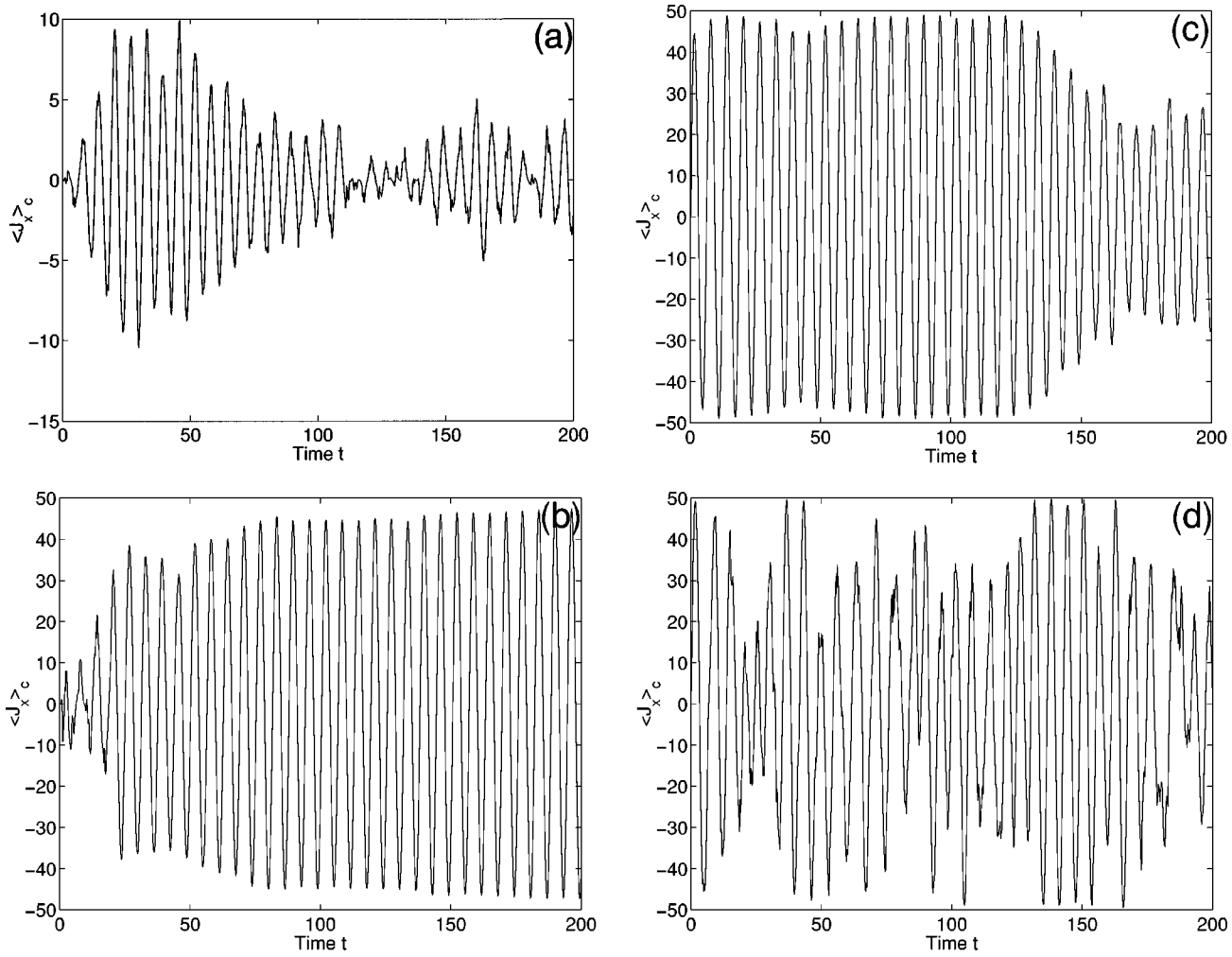

FIG. 3. Evolution of $\langle \hat{J}_x \rangle_c$ in the monitored system, for $N=100$ atoms and $\bar{\kappa}=0$. In (a), $\bar{\chi}=0.0001$, in (b), $\bar{\chi}=0.001$, (c), $\bar{\chi}=0.01$, and in (d), $\bar{\chi}=0.1$.

Thus we can see how the system evolution is conditioned upon the measured current.

Adiabatic elimination of the optical field, using Eq. (19) gives

$$d|\tilde{\Psi}_c(t)\rangle = dt\left[-i\hat{H}_2 - \frac{8\chi^2\epsilon^2}{\gamma^3}\hat{J}_x^2 + I(t)\hat{J}_x\right]|\tilde{\Psi}_c(t)\rangle, \tag{37}$$

$$I(t) = \frac{32\chi^2\epsilon^2}{\gamma^3}\langle \hat{J}_x\rangle_c + \frac{4\chi\epsilon}{\sqrt{\gamma^3}}\frac{dW}{dt}(t). \tag{38}$$

Hence the oscillations in the occupation number between the two wells can be determined from the measured current.

It is helpful to consider the Shrödinger equation for the *normalized* ket, which does not explicitly mention the detection current:

$$d|\Psi_c(t)\rangle = \left[-i\hat{H}_2 dt - \frac{8\chi^2\epsilon^2}{\gamma^3}(\hat{J}_x - \langle \hat{J}_x\rangle_c)^2 dt + \frac{4\chi\epsilon}{\sqrt{\gamma^3}}(\hat{J}_x - \langle \hat{J}_x\rangle_c)dW\right]|\Psi_c(t)\rangle. \tag{39}$$

The terms in the equation due to the measurement depend on the quantity $\hat{J}_x - \langle \hat{J}_x\rangle_c$. This is minimal in semiclassical type trajectories for which $\langle \hat{J}_x^2\rangle_c$ factorizes to $\langle \hat{J}_x\rangle_c^2$. Thus it may be expected that for some range of values of χ, the stochastic measurement terms would drive the system towards an oscillating trajectory for which $\langle \hat{J}_x^2\rangle_c \simeq \langle \hat{J}_x\rangle_c^2$.

IV. SIMULATIONS

The results of the simulations are shown in Figs. 2–5. Time is plotted along the x axis in dimensionless units (normalized by the inverse of the tunneling frequency Ω). The strengths of the atom-atom collisions and the atom-field interaction were controlled by varying the normalized variables $\bar{\kappa}=\kappa/\Omega$ and $\bar{\chi}=\chi\epsilon/\sqrt{\Omega\gamma^3}$. The parameters stated previously give the range of measurement strengths used in the simulations ($10^{-4}<\bar{\chi}<0.1$) when the power of the optical field is varied from 0.06 to 6 mW. The mass of the particles is taken to be $m=1.5\times10^{-25}$ kg.

The measured current gives the conditional dynamics of the the system. However, in the conditional results shown, we plot $\langle \hat{J}_x\rangle_c$, which is proportional to the current without the noise [Eq. (38)]. For clarity, the other moments, namely,

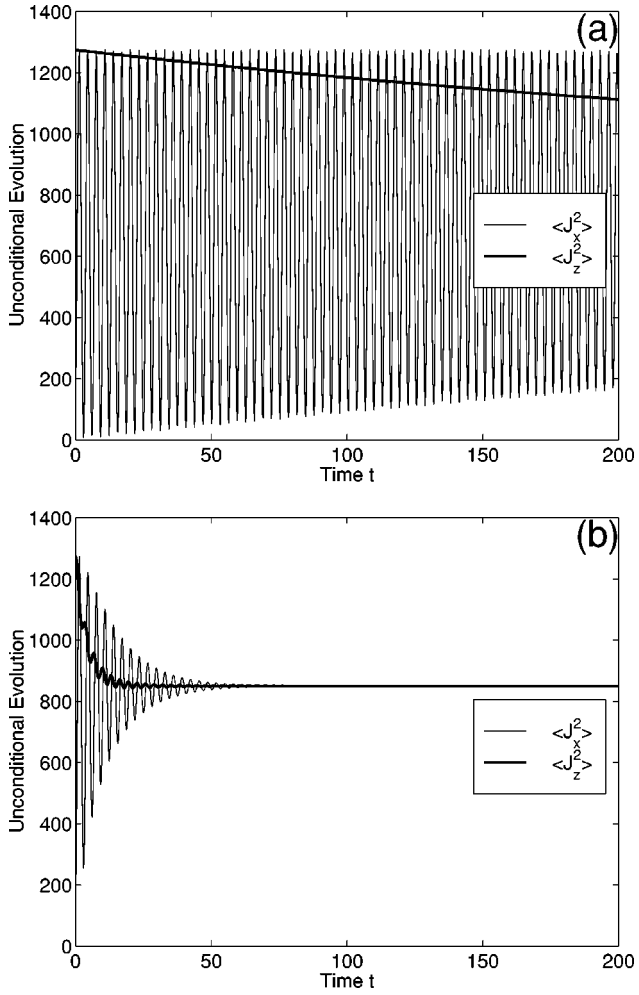

FIG. 4. Unconditional evolution of second-order moments, for $N=100$ atoms and $\bar{\kappa}=0$. In (a), $\bar{\chi}=0.01$, in (b), $\bar{\chi}=0.1$

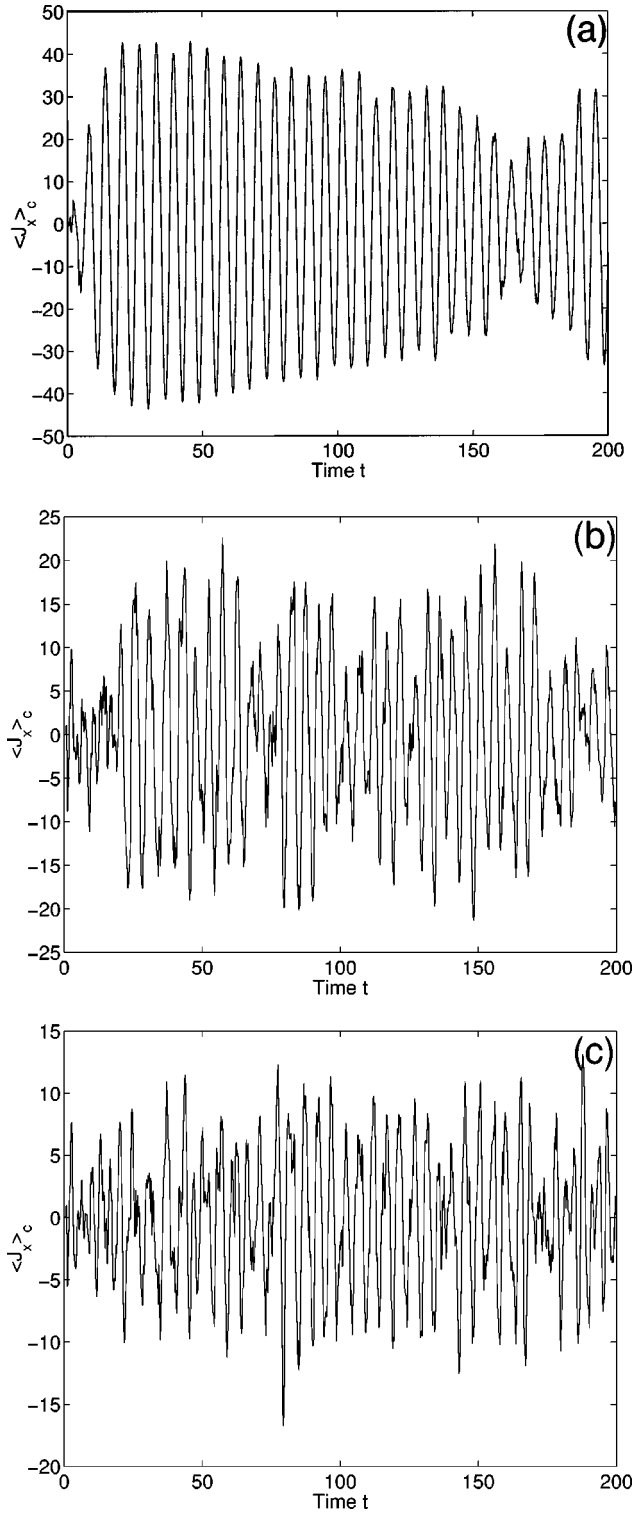

FIG. 5. Evolution of $\langle \hat{J}_x \rangle_c$ in the monitored system, for $N=100$ atoms, and $\bar{\chi}=0.001$. In (a), $\bar{\kappa}=0.0001$, in (b), $\bar{\kappa}=0.005$, and in (c) $\bar{\kappa}=0.02$.

$\langle \hat{J}_y \rangle_c$ and $\langle \hat{J}_z \rangle_c$, are not plotted in the figures. Except when κ is very large, $\langle \hat{J}_y \rangle_c$ follows $\langle \hat{J}_x \rangle_c$, but with a $\pi/2$ phase difference, and $\langle \hat{J}_z \rangle_c$ remains at or close to zero.

The dynamics of the unmonitored system when started with all the condensate in one well has been discussed in previous work [12]. Basically when there are no atom-atom interactions (i.e., $\bar{\kappa}=0$), $\langle \hat{J}_x \rangle$ oscillates from $-N/2$ to $+N/2$. When the interactions are present but only weak, tunneling still occurs, but the amplitude quickly collapses due to nonlinear dephasing. The collapse is followed some time later by small revivals. There is a critical strength of collisions ($\bar{\kappa}N=1$) at which the tunneling is suppressed. Above this value of $\bar{\kappa}$, the condensate is trapped in the well in which it started, with only very small oscillations occurring in $\langle \hat{J}_x \rangle$.

We expect to see similar behavior in the current of the monitored system [Eq. (39)]. When $\bar{\kappa}=0$, $\langle \hat{J}_x \rangle_c$ oscillates as before, for weak atom-light coupling (i.e., $\bar{\chi}N \simeq < 1$). For stronger measurements, the resulting backaction can be seen in the current. For long times, the amplitude of the tunneling oscillations starts to fluctuate and a slow phase change is evident. In the case when atom collisions are present, the effect of the measurements is to halt the collapse of the oscillations seen in the unmonitored system. The phase changes are also more pronounced. The effect of the critical value ($\bar{\kappa}N=1$) is seen in the suppression of the oscillations in the current above this value. Figure 2 shows the evolution of $\langle \hat{J}_x \rangle_c$ for values of $\bar{\kappa}$ above and below the critical value.

If the system is started with an equal number of atoms in each well, then we expect no coherent tunneling in the absence of any detection apparatus. However, the presence of

the field effects a measurement on the condensate system. This should establish a phase, which can be detected by measuring the output current $I(t)$. The simulations of Eq. (39) show an oscillation in the current and, for the optimum interaction strength, this can be established in a few tunneling periods, for a small number of atoms. The results for the case where there are no atom collision, i.e., $\bar{\kappa}=0$, are shown in Fig. 3, for various measurement strengths $\bar{\chi}$. The growth in oscillations occurs because, for large enough $\bar{\chi}$, $\langle \hat{J}_x \rangle_c^2$ is driven to match $\langle \hat{J}_x^2 \rangle_c$, which typically has large oscillations.

If, as in Figs. 3(a) and 3(b), the interaction strength is too small ($\bar{\chi}N \leqslant 0.1$), then generally the fluctuations are not large enough to drive full tunneling and the current suffers small, rather irregular oscillations. However, even for large $\bar{\chi}$, when the oscillations in the current are established, such as in Fig. 3(c), they are not guaranteed to stay large in amplitude. This is because $\langle \hat{J}_z^2 \rangle_c$ undergoes what appears to be a random walk, which, because of the Casimir invariant, directly affects the amplitude of the oscillations in $\langle \hat{J}_x^2 \rangle_c$ and $\langle \hat{J}_y^2 \rangle_c$. Consequently, since the measurement locks $\langle \hat{J}_x \rangle_c^2$ onto the orbit of $\langle \hat{J}_x^2 \rangle_c$, this changes the amplitude of the oscillations in the current. Because of the random nature of the orbit of $\langle \hat{J}_z^2 \rangle_c$, the tunneling oscillations in the current over a certain time frame in a ''good'' run may be large, but in another with the same parameters the oscillations may be small and irregular in amplitude.

When the measurement is quite strong ($\bar{\chi}N \simeq 10$), as in Fig. 3(d), the tunneling oscillations appear to be quite irregular. However, a Fourier transform of the current picks out the tunneling frequency Ω very strongly, so the fluctuations are mainly in the amplitude of oscillations, not so much in the phase. When the measurement strength is very large ($\bar{\chi}N = 40$), $\langle \hat{J}_x \rangle_c$ still indicates a tunneling from one well to another, but the oscillations are no longer harmonic and appear quite random, both in frequency and amplitude.

The equations for the *unconditional* dynamics [Eqs. (23)–(29)] show a decay in the oscillations of $\langle \hat{J}_x^2 \rangle$ and $\langle \hat{J}_y^2 \rangle$ for long times, which increases with the measurement strength $\bar{\chi}$. Figure 4 shows the unconditional dynamics for two different measurement strengths. No such decay is seen in the individual trajectories, but rather there is a diffusion in the phase of the oscillation over long times that accounts for the decay in the mean evolution. This change in phase appears to be most rapid over the periods when the oscillations are small in amplitude and most likely to suffer random fluctuations.

The presence of atom-atom interactions increases the phase diffusion, even for quite weak collisions ($\bar{\kappa}N \leqslant 0.1$). Figure 5 shows the evolution of $\langle \hat{J}_x \rangle_c$ for various atom-atom interaction strengths $\bar{\kappa}$, above and below the critical value. The amplitude is also more irregular, and the Fourier transform of the oscillations no longer shows a clear peak at the expected tunneling frequency, but a group of random spikes centered on the the tunneling frequency. In Fig. 5(b), $\bar{\kappa} = 0.005$, which is close to the value of $\bar{\kappa}$ calculated from the parameters given in previous sections. Above the critical value of $\bar{\kappa}N = 1$, $\langle \hat{J}_x \rangle_c$ suffers small, very irregular oscillations around the origin [Fig. 5(c)]. This is quite different from the behavior of $\langle \hat{J}_x \rangle_c$ when the condensate was initially placed entirely in one well [Fig. 2(b)], in which case the condensate was trapped in the well it started in and the critical value of $\bar{\kappa}$ marked quite a sharp boundary (or bifurcation) between two different types of behavior. In this case where the condensate is distributed equally between the wells, the condensate is trapped in neither well, but remains across both, and the change in behavior as the critical point is crossed is more continuous. As $\bar{\kappa}$ increases past the critical point, we see a decrease in the overall amplitude of the tunneling and in its regularity. However, the critical value of $\bar{\kappa}$ is still quite meaningful in this case an indication of when the strength of the atom collisions significantly suppresses the tunneling.

V. CONCLUDING REMARKS

We have shown that this homodyne detection scheme, for an appropriate choice of measurement strength χ, could well be suitable to detect the relative phase, in the form of Josephson-like tunneling, between two condensates in a double-well potential. The dynamics of the measured current reflect the tunneling of the condensate as well as the self-trapping effect caused by atom collisions. It also demonstrates quite vividly how a measurement can establish a (relative) phase in a system which initially exhibits no phase information.

ACKNOWLEDGMENT

The authors would like to thank H. M. Wiseman for useful discussions.

[1] M. H. Anderson, J. R. Ensher, M. R. Matthews, C. E. Wieman, and E. A. Cornell, Science **269**, 198 (1995).
[2] C. C. Bradley, C. A. Sackett, J. J. Tollett, and R. G. Hulet, Phys. Rev. Lett. **75**, 1687 (1995).
[3] K. B. Davies, M.-O. Mewes, M. R. Andrews, N. J. van Druten, D. S. Durfee, D. M. Kurn, and W. Ketterle, Phys. Rev. Lett. **75**, 3969 (1995).
[4] Reports on more recent experiments can be found on http://amo.phy.gasou.edu/bec.html
[5] J. Javanainen and S. M. Yoo, Phys. Rev. Lett. **76**, 161 (1996).
[6] J. I. Cirac, C. W. Gardiner, and P. Zoller, Phys. Rev. A **54**, R3714 (1996).
[7] M. W. Jack, M. J. Collett, and D. F. Walls, Phys. Rev. A **54**, R4625 (1996).
[8] J. Ruostekoski and D. F. Walls, Phys. Rev. A **56**, 2996 (1997).
[9] J. Ruostekoski, M. J. Collett, R. Graham, and D. F. Walls, Phys. Rev. A **57**, 511 (1998).
[10] S. M. Barnett, K. Burnett, and J. A. Vaccaro, J. Res. Natl. Inst.

Stand. Technol. **101**, 593 (1996).
[11] R. Graham, T. Wong, M. J. Collett, S. M. Tan, and D. F. Walls, Phys. Rev. A **57**, 493 (1998).
[12] G. J. Milburn, J. F. Corney, E. M. Wright, and D. F. Walls, Phys. Rev. A **55**, 4318 (1997).
[13] See, for example, *Bose Einstein Condensation*, edited by A. Griffin, D. W. Snoke, and S. Stringari (Cambridge University Press, Cambridge, 1995).
[14] G. J. Milburn, K. Jacobs, and D. F. Walls, Phys. Rev. A **50**, 5256 (1994).
[15] H. M. Wiseman and G. J. Milburn, Phys. Rev. A **47**, 642 (1993).
[16] H. M. Wiseman, Ph.D. thesis, University of Queensland, 1994, p. 51.